Journal of Ceramic Processing Research. Vol. 18, No. 7, pp. 550~553 (2017)

J O U R N A L O F
Ceramic Processing Research

Preparation of $(Pb_{0.52}Zr_{0.48})TiO_3$ Thin Films On $PbTiO_3$ Seed Layer

Jong Cheol Kim[a], Kyoung Ryeol Park[b], Jae Eun Jeon[b], Jung-Il Lee[c] and Jeong Ho Ryu[c,*]

[a]*Department of Materials Science and Engineering, Korea University, Seoul 02841, Korea*

[b]*Department of Materials Science and Engineering, Hanyang University, Seoul 04763, Korea*

[c]*Department of Materials Science and Engineering, Korea National University of Transportation, Chungju, Chungbuk 27469, Korea*

$(Pb_{0.52}Zr_{0.48})TiO_3$ (PZT) thin films were prepared on $PbTiO_3$ (PT) seed layers by chemical solution deposition. PT layer with 50 nm was used as seed layer to transfer 100 texture to PZT thin films by heterogeneous nucleation during heat treatment. Highly 100 textured PZT thin films were obtained after heat treatments at 700 °C confirmed by X-ray diffraction data. The prepared PZT thin films show the thickness of 350 nm with 50 nm PT seed layer. Based on the EDX line profile of PZT, Zr/Ti ratio was slightly different inside PZT films, which suggests that interdiffusion of Ti and Zr occurs across the films during heat treatments. Also, nanobeam diffraction patterns reveals that PZT and PT seed layer are tetragonal perovskite phases without any secondary phases.

Key words: PZT thin film, Seed layer, Interdiffusion, Zr/Ti ratio, Perovskite phases.

Introduction

$(Pb_{0.52}Zr_{0.48})TiO_3$ (PZT) thin film has been actively studied due to its excellent piezoelectric and ferroelectric properties for the application of energy harvesting, capacitors and microsensors [1-3]. Different piezoelectric and ferroelectric properties of the PZT thin films can be obtained with control of the crystallographic texture. For example, 111 textured PZT thin films can show lower coercive field (E_c), while 100 textured PZT thin films shows the highest piezoelectric coefficient [4-7]. Therefore, various processing approach towards the formation of crystallographic texture on PZT thin films has been explored [8].

$PbTiO_3$ (PT) thin films with the thickness below 100 nm are often used as a seed layer to promote 100 texture in the PZT thin film [9-11]. Also, it is well known that such a seed layer is helpful to prevent the interdiffusion between the substrate and thin films during post annealing [12]. Both PT seed layers and PZT thin films are usually prepared by chemical solution deposition (CSD) consisted of solution preparation, spin coating and heat treatments including pyrolysis (~ 450 °C) and crystallization (~ 750 °C) [12]. During heat treatments, the thin films after pyrolysis are similar to an amorphous layer and then, following heat treatments at high temperature lead to the crystallization of the perovskite PT and PZT thin films [13]. Simultaneously, diffusion of different elements such as Ti, Zr and Pb occurs inside the films, which results in the compositional segregation in the thin films. For instance, Pb in the amorphous layer after pyrolysis can diffuse into platinum (Pt) electrodes and then, reacts with the Pt electrode for the formation of intermetallic Pt_xPb phase [13]. Although Pt_xPb often disappears with elevated temperature during heat treatments above 450 °C, potential interdiffusion between PT seed layer and PZT during heat treatments can result in an undesired composition of PZT thin films.

In this study, the effect of PT seed layer on the crystallization of PZT thin films is studied. Crystal structure of the PZT thin films was analyzed after heat treatments. Also, the formation of the crystallographic texture and elemental distribution in PZT thin films is discussed based on the EDX line profile and nanobeam pattern using transmission electron microscopy.

Experimental Procedure

A 30% Pb excess PT solution was deposited on the Pt electrode via the chemical solution deposition (CSD) method based on the work of Muralt et al. [14]. The Pt electrode was consisted of $Si/SiO_2/TiO_2/Pt$. Preparation of the PT solution is as follows; Lead acetate trihydrate was mixed 2-methoxyethanol (2-MOE) into the flask. In another flask, Ti isopropoxide with 2-MOE was mixed using stir bar while vacuum distillation was performed on the lead acetate solution using a rotary evaporator. After the vacuum distillation of the lead acetate solution, the Ti isopropoxide solution was added to the lead acetate solution in the glove box. Additional vacuum distillation was performed. The PT solution was spincoated for 45 s at a speed of 3,000 rpm and then

*Corresponding author:
Tel : +82-43-841-5384
Fax: +82-43-841-5380
E-mail: jhryu@ut.ac.kr

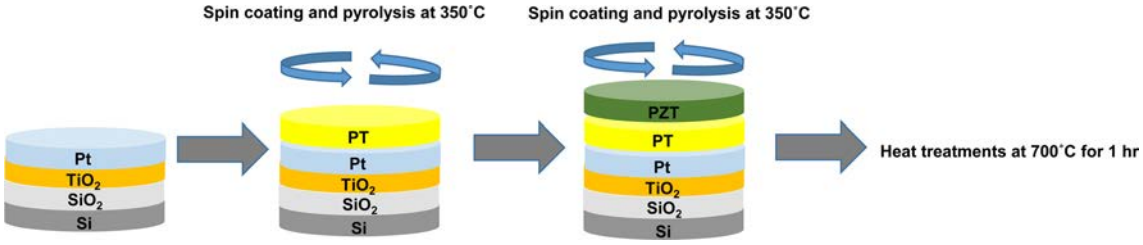

Fig. 1. Illustration of preparation of PZT thin films and PT seed layer on Pt substrates.

pyrolyzed at 350 °C for 2 min on a hot plate. Crystallization of pyrolyzed PT was performed at 700 °C for 60 s using a rapid thermal annealing (RTA). This PT layer was used as a seed layer for 2-MOE PZT thin films.

PZT solutions with a 5% Pb excess were prepared based on Budd et al. [15]. Lead trihydrate and 2-MOE solvent were mixed in flask inside a glove box to make lead acetate solution. Vacuum distillation was conducted on the flask using a rotary evaporator. The flask with lead acetate solution was located on 120 °C silicon oil bath. and rotated at 120 rpm under nitrogen atmosphere. After Nitrogen gas was turned off, a flask was depressurized and rotated for 20 min. During rotation of the flask on the silicon oil bath, water vapor and 2-MOE solvent was evaporated and then condensed into cooling coils. The condensed drops were collected in a collection flask under the cooling coils. When the lead acetate solution turned white foam under rotation, the velocity of rotation was decreased to 35 rpm and the flask was raised out of the silicon oil bath. Nitrogen gas was applied into the flask to remove vacuum. The flask was removed from the evaporator and submerged in water until room temperature. Prior to the vacuum distillation of lead acetate solution, Ti iso-propoxide and 2-MOE were poured into another flask and sealed inside the glove box. The Ti and Zr precursors in 2-MOE were mixed using stir bar. An additional 2-MOE was added into the Ti/Zr solution and then poured into lead acetate solution inside glove box.

This step was repeated one more time. The flask was moved to the evaporator for vacuum distillation. The flask was placed in a silicon oil bath preheated at 120 °C and rotated at 120 rpm for 4 h. A vacuum was applied into the flask for 5 min after 4 h and then nitrogen gas was applied for 5 min. PZT solution was spin coat on the PT seed layer at a speed of 2000 rpm for 45 s and then pyrolyzed at 350 °C for 2 min on a hot plate. The spin coating and pyrolysis sequence was repeated twice, for a total of three pyrolysis treatments per sample. After pyrolysis, the PZT thin films were annealed at 700 °C for 1 hr with heating rate with 5 °C/min. PZT thin films on PT seed layer is illustrated in Fig. 1.

X-ray diffraction (XRD) patterns of the prepared PZT thin films were recorded for analysis of crystal structure of PT and PZT thin films. Dark field cross-sectional images, nano-beam diffraction (NBD) patterns and EDX line profiles of PZT on the PT seed layer after crystallization were examined using transmission electron microscopy (TEM). Sample preparation including thinning, milling and lift-out for TEM analysis was conducted using the focused ion beam (FIB) [16].

Results and Discussion

XRD patterns of the PT seed layer, and PZT thin films after crystallization are shown in Fig. 2. The (001), (100), (002) and (200) peaks of the PT seed layer corresponding to 21.66, 22.42, 44.48, and 46.02 ° were observed, which implies that PT seed layer has high 100 texture with tetragonal perovskite phase as shown in Fig. 2(a). Also, peak intensity of (100) is higher than that of (001) in PT seed layer. In Fig. 2(b), after crystallization of PZT thin films at 700 °C, mainly, (001), (100), (002) and (200) peaks were observed with small amount of (110) and (210), which can support that 100 textured PT seed layer as a template nucleates the 100 texture in PZT thin films. Interestingly, peak intensity of (001) of PZT thin films is stronger than that of PT seed layer. It is noted that (001) of the PZT can be nucleated from the (100) of cubic phase PT seed layer which is induced by phase transition of PT from tetragonal to cubic phase above curie temperature around 450 °C. [12] Such a phase transition of PT seed layer can lead to nucleation and growth of 100 texture along c axis in PZT thin films.

A cross-sectional micrograph of a PZT thin film after heat treatments at 700 °C in Fig. 3(a) shows two distinct regions on the Pt substrates which are crystalline PT and PZT layer. The thickness of the PT

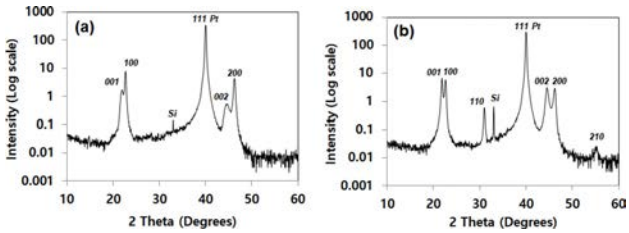

Fig. 2. XRD patterns of (a) PT seed layer and (b) PZT thin films after heat treatments.

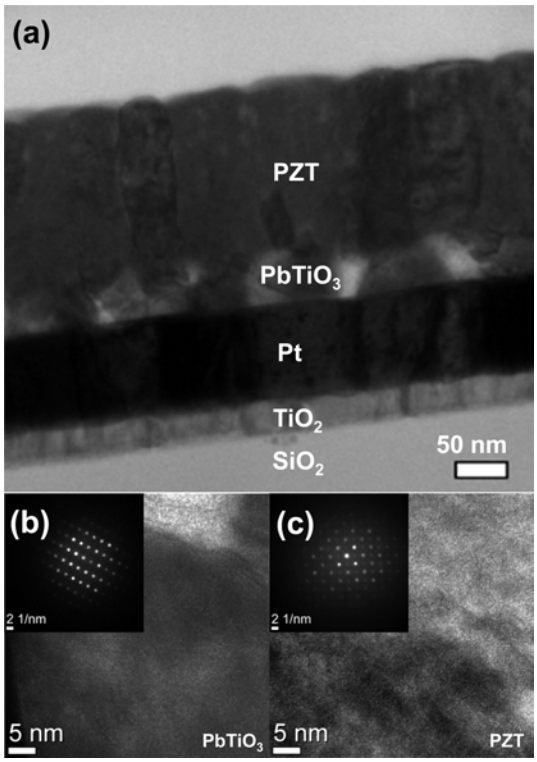

Fig. 3. (a) Cross section view of PZT and PT seed layer on Pt substrates, NBD patterns of (b) PZT thin films and (c) PT seed layer, and (d) EDX line profile of PZT thin films on PT seed layer.

and PZT were 50 and 350 nm, respectively. Also, PZT has columnar structure, which can be an evidence that 100 texture of the PZT can be originated from PT seed layer. The interfacial roughness was observed between the PT layer and PZT layer, which might be attributed to several factors such as dewetting or interdiffusion during crystallization. Nanobeam diffraction patterns (NBD) of PT and PZT are shown in Fig. 3(b) and (c), respectively. Both PT and PZT are tetragonal perovskite phase without any amorphous phase, which implies that PT and PZT thin films are fully crystallized under the conditions of heat treatments.

EDX line profiles of Pb, Ti and Zr are provided in Fig. 4. Pb, Ti and Zr were not observed in the Pt layer. When PZT thin films are deposited on Pt substrates without any seed layer, Pb diffuses easily into Pt substrates and subsequently, formation of intermetallic Pt_xPb occurs at temperature between 300 and 500 °C during heat treatments [13]. Pb in Pt_xPb phase can be reoxidized and re-diffuses into PZT thin films at further heating above 500 °C. However, remained Pb in Pt substrates is commonly observed after processing, which can deteriorate the electrical properties of the PZT thin films [17]. Therefore, no observation of Pb in Pt substrates after crystallization of PZT thin films indicates that no interdiffusion of elements between the substrate and the upper PT/PZT layers has occurred.

A small amount of elemental Zr was detected in the PT layer and a similar amount of elemental Pb was detected in both the PT and PZT layers, which suggests that Zr from the PZT layer diffused into PT layer and Ti rich PZT was crystallized near the Pt substrates. Also, a decrease in the Ti and a similar increase in the Zr with increasing distance were observed in the PZT layer, which implies that the Zr/Ti molar ratio increased throughout the cross-section from the Pt-thin film interface to the surface with increasing temperature. The average Zr/Ti ratios in the entire PT and PZT layer were calculated as 10/90 and 51/49, which does not correspond to the initial stoichiometry of the thin films before crystallization.

The crystallization of Ti rich PZT appears to occur at a lower crystallization temperature, followed by the formation of Zr rich PZT across the thin film. It has been reported that dominant 100 texture is commonly observed in Zr rich PZT thin films [18]. Higher temperature is required to crystallize PZT with increasing Zr concentration, which leads to homogeneous nucleation in PZT thin films [19]. In the case of PZT, the (100) has the lowest surface energy, and thereby dominant nucleation and growth of 100 texture occur. [20] Dominant 100 texture for interdiffusion between the PT layer and PZT layer leads to increased Zr concentration towards surface and increased Ti concentration towards

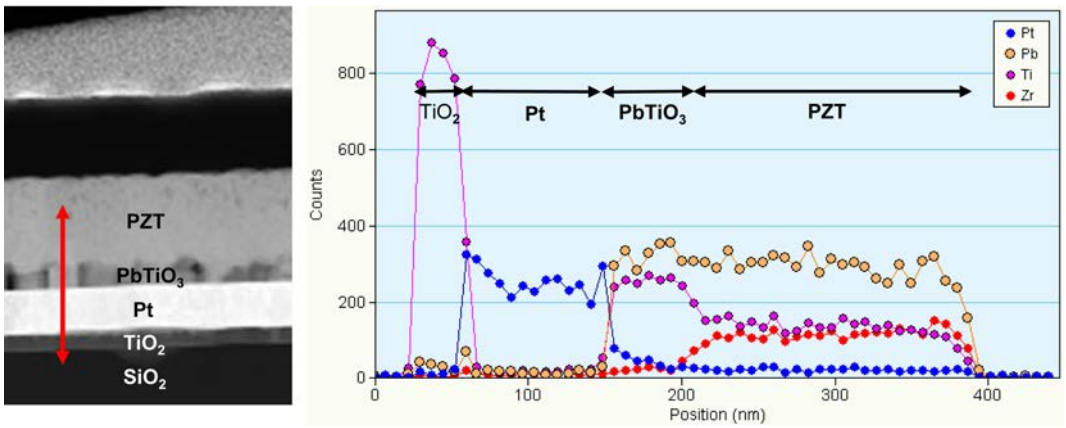

Fig. 4. EDX line profiles of Pb, Ti and Zr of PZT and PT seed layer on Pt substrates.

the PT-PZT interface, which promotes PZT thin films with a higher Zr concentration.

Conclusions

The effect of PT seed layer on the crystallization behavior of PZT thin films was investigated. Crystallized PZT thin films show highly 100 texture with tetragonal perovskite phase, which can be induced by 100 texture of the PT seed layer. During the crystallization of PZT thin films, PT seed layer can be a diffusion barrier for Pb from PZT thin films to Pt substrates. Additionally, formation of a Ti rich PZT layer occurs near PT seed layer through diffusion of Zr atoms from the PZT layer to the PT layer. It is suggested that interdiffusion of Ti and Zr occurs between PT and PZT during the crystallization, which can lead to chemical gradients in PZT thin films.

Acknowledgments

This research was supported by Basic Science Research Program through the National Research Foundation of Korea (NRF) funded by the Ministry of Education (No. 2016R1D1A3B03933765).

References

1. J.R. Bronson, J.S. Pulskamp, R.G. Polcawich, C.M. Kroninger, and E.D. Wetzel, "PZT MEMS actuated flapping wings for insect-inspired robotics"; pp. 1047–1050 in IEEE 22nd International Conference on Micro Electro Mechanical Systems, Jan 25-29 2009. MEMS (IEEE Xplore, 2009), 2009.
2. Y. Takahashi and M. Suzuki, "Piezoelectric ink jet printer head"; U.S. Patent No. 5 266 964, 1993.
3. N. Ledermann, P. Muralt, J. Baborowski, S. Gentil, K. Mukati, M. Cantoni, A. Seifert, and N. Setter, Sens. Actuators A Phys. 105 (2003) 162-170.
4. G.L. Brennecka, J.F. Ihlefeld, J.P. Maria, B.A. Tuttle, and P.G. Clem, J. Am. Ceram. Soc. 93 (2010) 3935-3954.
5. B.A. Tuttle, J.A. Voigt, T.J. Garino, D.C. Goodnow, R.W. Schwartz, D.L. Lamppa, T.J. Headley, and M.O. Eatough, Eight IEEE international symposium on applications of ferroelectrics, Greenville, SC, USA (1992).
6. R.W. Whatmore, Q. Zhang, C.P. Shaw, R.A. Dorey, J.R. Alcock, Phys. Scripta (2007) T129.
7. G.L. Smith, J.S. Pulskamp, L.M. Sanchez, D.M. Potrepka, R.M. Proie, T.G. Ivanov, R.Q. Rudy, W.D. Nothwang, S.S. Bedair, C.D. Meyer, and R.G. Polcawich, J. Am. Ceram. Soc. 95(6) (2012) 1777-1792.
8. P. Muralt, M. Kohli, T. Maeder, A. Kholkin, K. Brooks, N. Setter, and R. Luthier, Sensor. Actuat. A 48 (1995) 157-165.
9. S. Hiboux, P. Muralt, and N. Setter, Proc. MRS, 596 (1999) 499.
10. G.L. Smith, J.S. Pulskamp, L.M. Sanchez, D.M. Potrepka, R.M. Proie, T.G. Ivanov, R.Q. Rudy, W.D. Nothwang, S.S. Bedair, C.D. Meyer, and R.G. Polcawich, J. Am. Ceram. Soc. 95(6) (2012) 1777-1792.
11. Y. Lin, B.R. Zhao, H.B. Peng, B. Xu, H. Chen, F. Wu, H.J. Tao, Z.X. Zhao, and J.S. Chen, Appl. Phys. Lett. 73 (1998) 2781.
12. S. Mhin, K. Nittala, C. Cozzan, K. Kim, D.S. Robinson, L.M. Sanchez, R.G. Polcawich, J.L. Jones J. Am. Ceram. Soc. 98(5) (2015) 1407-1412.
13. S. Mhin, C. Cozzan, K. Nittala, P. Wanninkhof, J.F. Ihlefeld, G.L. Brennecka, 96(9) (2013) 2706-2709.
14. P. Muralt, T. Maeder, L. Sagalowicz, S. Hiboux, S. Scalese, D. Naumovic, R. G. Agostino, N. Xanthopoulos, H. J. Mathieu, L. Patthey, and E. L. Bullock, J. Appl. Phys. 83 (1998) 3835.
15. K.D. Budd, S.K. Dey, and D.A. Payne, Br. Ceram. Proc. 36 (1985) 107-121.
16. [R.H. Kim, W.S. Ahn, S.H. Han, and S.K. Choi, Appl. Phys. Lett. 90 (2007) 172907.
17. J. Zhong, V. Batra, H. Han, S. Kotru, and R.K. Pandey, J. Vac. Sci. & Tech. A33 (5) (2015) 05E119.
18. S.Y. Chen and I.W. Chen, J. Am. Ceram. Soc. 81 (1998) 97-105.
19. A.P. Wilkinson, J.S. Speck, A.K. Cheetham, S. Natarajan, and J.M. Thomas, Chem. Mater. 6 (1994) 750-754.
20. A. Bose, PZT Thin Film Growth and Chemical Composition Control on Flat and Novel Three-Dimensional Micromachined Structures for MEMS Devices, Ph. D dissertation, École Polytechnique Federale de Lausanne (2011).